

NASA TECHNICAL NOTE



NASA TN D-5181

C.1

LOAN COPY: RETURN
AFWL (WLIL-2)
KIRTLAND AFB, N ME

0131823



TECH LIBRARY KAFB, NM

NASA TN D-5181

ABSORPTION OF INFRARED RADIATION BY ICE CRYODEPOSITS

by Stephen V. Pepper
Lewis Research Center
Cleveland, Ohio



0131823

ABSORPTION OF INFRARED RADIATION BY ICE CRYODEPOSITS

By Stephen V. Pepper

Lewis Research Center
Cleveland, Ohio

NATIONAL AERONAUTICS AND SPACE ADMINISTRATION

For sale by the Clearinghouse for Federal Scientific and Technical Information
Springfield, Virginia 22151 - CFSTI price \$3.00

ABSTRACT

The absorption of isotropic 300 K blackbody radiation by ice cryodeposits is analyzed theoretically. The analysis is based on the hypothesis that the cryodeposit reflects infrared radiation specularly. The effects of interfering and noninterfering multiply reflected waves are investigated. The main results of the analysis are predictions of the absorptance as a function of cryodeposit thickness. The effect of interference is to lower the cryodeposit absorptance for thicknesses less than 2 micrometers. Reasonably good agreement with available experimental data has been achieved over a wide range of thicknesses (0.2 to 400 μm).

ABSORPTION OF INFRARED RADIATION BY ICE CRYODEPOSITS

by Stephen V. Pepper

Lewis Research Center

SUMMARY

The absorption of isotropic 300 K blackbody radiation by ice cryodeposits on metal substrates is analyzed theoretically. The analysis is based on the hypothesis that the cryodeposit reflects the incident radiation specularly. This specular model is developed using the equations of classical thin-film optics. The effects of both interfering and noninterfering waves is investigated.

The analysis gave three main results: (1) The absorptance was essentially independent of substrate reflectance and cryodeposit thickness for thicknesses greater than 100 micrometers. (2) For large cryodeposit thicknesses ($> 20 \mu\text{m}$) on highly reflective substrates, the absorptance varies inversely with cryodeposit density, while for thicknesses less than 20 micrometers, the absorptance varies directly with cryodeposit density. (3) Interference effects are important for thicknesses less than 4 micrometers. At these thicknesses, the effect of interference is to lower the absorptance below that which would be obtained for the noninterference case.

A comparison of the predicted absorptances with the available experimental data yielded reasonable agreement both in magnitude and trends. However, the comparison illustrates quite clearly the need for more accurate optical constants to determine the mechanisms responsible for the experimental data. In addition, new experiments are required to investigate interference effects, the effect of surface roughness, and, finally, the degree of specularity achieved by a cryodeposit.

INTRODUCTION

The effect of cryogenic condensates (cryodeposits) on the operation of space simulation chambers has been of interest for some time. Cryodeposits that form on the cryogenically cooled shrouds in the interior of a space simulator consist mainly of solid films of carbon dioxide and water. These deposits change the solar and infrared ab-

sorptance and reflectance of the shroud, thus altering the thermal environment of a test model.

Cryodeposits may also form on the walls of cryogenic storage tanks in space. Therefore, the absorptance of radiation by the tank, and thus the boiloff rate of the cryogen, will depend on the radiative properties of the cryodeposit. If the tank is shielded from various sources of radiation by shadow shields, the efficiency of shielding will depend on whether cryodeposits are present and the nature of their radiative properties.

A number of investigations (refs. 1 to 4) have been conducted to measure the solar or infrared absorptance or reflectance of cryodeposits on different substrates. The main objective of these investigations was to obtain the absorptance or reflectance as a function of cryodeposit thickness. In particular, the absorptance of 300 K, isotropic, blackbody radiation by water and carbon dioxide cryodeposit films between 0.1 and 200 micrometers thick has been measured by Caren, Gilcrest, and Zierman (ref. 2), Young and Todd (ref. 3), and, most recently, by Merriam (ref. 4).

Previous attempts (refs. 2 to 4) to understand these experiments have utilized the equations of radiative transfer in a scattering and absorbing medium. In this approach, the interest is mainly on the cryodeposit defects such as voids and rough interfaces which scatter the incident radiation. Such an analysis has proved valuable in understanding the reflectance of visible light by cryodeposits. However, radiative properties of cryodeposits are affected by both the scattered and specular components of the reflected radiation. At present, it is not clear which component determines the behavior of cryodeposits for incident infrared radiation. It is therefore of interest to investigate analytically whether the understanding can be enhanced by a specular analysis.

An additional reason for performing a specular analysis is that it furnishes a rigorous theoretical prediction that is a limiting case, valid in the absence of scattering. Any deviation from the specular prediction can then be attributed to the effects of cryodeposit defects. Furthermore, another important reason for making a specular analysis is that the effects of wave interference, which are not easily incorporated into the equations of radiative transfer, can be considered.

After the analysis presented herein was completed, Merriam (ref. 4) presented an analysis approaching the problem using the general equations of radiative heat transfer. In the absence of scattering, his analysis reduced to the specular theory without wave interference. However, there are sufficient differences and interest in the two approaches to warrant additional discussion. In particular, effects resulting from the interference of multiply reflected waves within the cryodeposit are discussed herein.

Only ice cryodeposits are studied because the numerical evaluation of the theoretical expressions requires a knowledge of the infrared optical constants of the cryodeposits. The infrared optical constants of solid carbon dioxide are not available.

The experiments that are analyzed were reported by Caren et al. (ref. 2) and Merriam (ref. 4). Their cryodeposits were vapor deposited on the walls of a calorimeter tank at 77 K. The measured absorptance was defined as the ratio of the energy absorbed by a boiling liquid in a calorimeter tank to the radiant energy incident on the tank. An analysis of the calorimeter energy balance shows that this measured absorptance is essentially 1 minus the reflectance of the cryodeposit-substrate complex (hereinafter referred to simply as the cryodeposit complex). Therefore, the analysis presented herein derives the reflectance of the cryodeposit complex as a function of cryodeposit thickness. The results of the theory are then compared with the experimental data of Caren et al. and Merriam.

SYMBOLS

\mathcal{A}	cryodeposit absorptance
d	cryodeposit thickness
J	spectral distribution function for incident radiation
K	component of propagation vector of electromagnetic field normal to surface
k	extinction coefficient
n	index of refraction
\hat{n}_1	complex index of refraction of cryodeposit
\hat{n}_2	complex index of refraction of substrate
R	amplitude reflectance coefficient for cryodeposit
\mathcal{R}	cryodeposit reflectance
r_1	Fresnel amplitude reflectance coefficient for vacuum-cryodeposit interface
r_2	Fresnel amplitude reflectance coefficient for cryodeposit-substrate interface
T	absolute temperature of radiation source
δ	dK_1
λ	wavelength of incident radiation
σ	Stefan-Boltzmann constant
θ	angle of incidence
ξ	$\sin^2 \theta$

Subscripts:

- p polarization parallel to plane of incidence
- s polarization perpendicular to plane of incidence

REFLECTANCE MODEL OF CRYODEPOSIT

The model developed is the simplest one possible: The cryodeposit is assumed to be a specularly reflecting film on a specular substrate. The radiation scattered by cryodeposit defects, such as voids and rough interfaces, is assumed to be negligible relative to the radiation specularly reflected. This model is the starting point of the analysis of the reflecting properties of any film system and may be rigorously developed.

A specular analysis of the reflectance must consider the possibility of interference between the multiply reflected waves in the film. The magnitude of interference effects depends on the thickness of the film and the effect of surface irregularities. Interference effects in films are usually important if the wavelength of the incident radiation is of the same order of magnitude as the film thickness. The incident 300 K blackbody radiation has essentially all its energy concentrated in the wavelength interval from 2 to 200 micrometers. Since the film thicknesses used in the experiments under consideration ranged between 0.1 and 200 micrometers, the possibility of interference between the multiply reflected waves was investigated.

Although interface irregularities have already been assumed to give rise to a negligible amount of scattered radiation, they can still serve to randomize the phase relations between the multiply reflected waves and thus diminish interference effects. However, the importance of these irregularities for interference phenomena decreases as the film thickness decreases (refs. 5 and 6). Thus, interference effects should be present for thin film thicknesses less than some given thickness. Unfortunately, the lack of information about the interface profiles makes it impossible to state a precise thickness for which interference becomes important. Under these circumstances, analysis of the film reflectance based on both interfering and noninterfering waves is necessary. If the theoretical predictions of the two cases differ greatly enough, a comparison with experimental data may decide whether or not interference takes place.

THEORETICAL ANALYSIS

The total absorptance of isotropic blackbody radiation by a cryodeposit complex is given by

$$\mathcal{R}(d) = 1 - R(d)$$

where $R(d)$ is the total reflectance of a cryodeposit complex of thickness d . Comparison with experiment requires an analytic expression for the total reflectance $R(d)$ to be derived. For this purpose, the incident radiation is analyzed into a spectral and spatial distribution of plane waves. The reflectance of these plane waves by an absorbing thin-film system will then be obtained and integrated over the angle of incidence and wavelength to obtain $R(d)$.

Consider first the spectral distribution of the incident radiation and let $J(\lambda)$ be the spectral energy distribution function. Then, the total reflectance is given by

$$R(d) = \frac{\int_0^\infty J(\lambda) R(d, \lambda) d\lambda}{\int_0^\infty J(\lambda) d\lambda} \quad (1)$$

where $R(d, \lambda)$ is the reflection coefficient for incident isotropic monochromatic radiation at wavelength λ .

The monochromatic radiation may be further analyzed into an angular distribution of plane waves. One such plane wave is depicted in figure 1. If $\xi = \sin^2\theta$, the spectral reflection coefficient $R(d, \lambda)$ is given by

$$R(d, \lambda) = \int_0^1 R(d, \lambda, \xi) d\xi \quad (2)$$

where $R(d, \lambda, \xi)$ is the reflection coefficient for a monochromatic plane wave of wavelength λ incident on the cryodeposit complex at an angle θ .

The expression for the total reflectance thus becomes

$$R(d) = \frac{\int_0^\infty J(\lambda) \int_0^1 R(d, \lambda, \xi) d\xi d\lambda}{\int_0^\infty J(\lambda) d\lambda} \quad (3)$$

The analysis will only consider incident blackbody radiation at temperature T so that

$$J(\lambda) = \frac{3.7413 \times 10^4}{\lambda^5} \frac{1}{\exp\left(\frac{14388}{\lambda T}\right) - 1}, \text{ W/(cm}^2\text{)(}\mu\text{m)}$$

and

$$\int_0^{\infty} J(\lambda) d\lambda = \sigma T^4$$

where $\sigma = 5.6687 \times 10^{-12}$ watt per square centimeter per K^4 is the Stefan-Boltzmann constant. In the expression for $J(\lambda)$, λ is in micrometers and T in kelvin. The expression for the total reflectance is then

$$\mathcal{R}(d) = \frac{6.5999 \times 10^{15}}{T^4} \int_0^{\infty} \frac{1}{\left[\exp\left(\frac{14\,388}{\lambda T}\right) - 1 \right] \lambda^5} \int_0^1 \mathcal{R}(d, \lambda, \xi) d\xi d\lambda \quad (4)$$

The equations that describe the reflection of monochromatic plane waves by an absorbing thin-film system are well known. The formulation used here is that given by Stern (ref. 7), which takes into account the extinction coefficient in both the film and the substrate. The usual convention for polarized waves is used: the subscript s denotes quantities associated with plane waves whose electric vector vibrates normal to the plane of incidence; the subscript p denotes quantities associated with plane waves whose electric vector vibrates parallel to the plane of incidence. The incident radiation is unpolarized, and, therefore,

$$\mathcal{R}(d, \lambda, \xi) = 0.5 [\mathcal{R}_s(d, \lambda, \xi) + \mathcal{R}_p(d, \lambda, \xi)]$$

Interfering Waves

For interfering waves, the reflection coefficients are given by

$$\mathcal{R}_s(d, \lambda, \xi) = |R_s(d, \lambda, \xi)|^2$$

and

$$\mathcal{R}_p(d, \lambda, \xi) = |R_p(d, \lambda, \xi)|^2$$

where R_s and R_p are amplitude reflectance coefficients. The expressions for R_s and

R_p are obtained by defining the Fresnel amplitude reflectance coefficients for the vacuum-ice and ice-substrate interfaces, respectively,

$$r_{1s} = \frac{K_0 - K_1}{K_0 + K_1}$$

$$r_{2s} = \frac{K_1 - K_2}{K_1 + K_2}$$

and

$$r_{1p} = \frac{\hat{n}_1^2 K_0 - K_1}{\hat{n}_1^2 K_0 + K_1}$$

$$r_{2p} = \frac{\hat{n}_2^2 K_1 - \hat{n}_1^2 K_2}{\hat{n}_2^2 K_1 + \hat{n}_1^2 K_2}$$

where

$$K_0 = \frac{2\pi}{\lambda} \cos \theta$$

$$K_1 = \frac{2\pi}{\lambda} \left(\hat{n}_1^2 - \xi \right)^{1/2}$$

$$K_2 = \frac{2\pi}{\lambda} \left(\hat{n}_2^2 - \xi \right)^{1/2}$$

$$\hat{n}_1 = n_1(\lambda) + ik_1(\lambda)$$

and

$$\hat{n}_2 = n_2(\lambda) + ik_2(\lambda)$$

The quantities K_0 , K_1 , and K_2 are the y-components of the propagation vectors of the plane waves in vacuum, ice, and substrate, respectively. In the expressions for K_1 and K_2 , the positive square root must be taken. The wavelength dependent complex indices of refraction of the film and substrate are denoted as \hat{n}_1 and \hat{n}_2 , respectively; $n(\lambda)$ is the index of refraction, and $k(\lambda)$ is the extinction coefficient at wavelength λ .

With the preceding definitions, the amplitude reflectance coefficients R_s and R_p may be written as

$$R_s(d, \lambda, \xi) = \frac{r_{1s} + r_{2s} e^{2i\delta}}{1 + r_{1s} r_{2s} e^{2i\delta}} \quad (5a)$$

$$R_p(d, \lambda, \xi) = \frac{r_{1p} + r_{2p} e^{2i\delta}}{1 + r_{1p} r_{2p} e^{2i\delta}} \quad (5b)$$

where $\delta = dK_1$. It may be shown that the limit of equations (5), as d approaches zero, yields the correct single surface Fresnel coefficient for a bare substrate.

Noninterfering Waves

For the case in which the multiply reflected waves do not interfere, the reflectance coefficients \mathcal{R}_s and \mathcal{R}_p are given by

$$\mathcal{R}_s(d, \lambda, \xi) = \frac{|r_{1s}|^2 + |r_{2s}|^2 (1 - 2 \Re e r_{1s}^2) \exp(-4 \Im m \delta)}{1 - |r_{1s}|^2 |r_{2s}|^2 \exp(-4 \Im m \delta)} \quad (6a)$$

$$\mathcal{R}_p(d, \lambda, \xi) = \frac{|r_{1p}|^2 + |r_{2p}|^2 (1 - 2 \Re e r_{1p}^2) \exp(-4 \Im m \delta)}{1 - |r_{1p}|^2 |r_{2p}|^2 \exp(-4 \Im m \delta)} \quad (6b)$$

In equations (6), $\Re e$ denotes the real part of a quantity and $\Im m$ denotes the imaginary part of a quantity. For the special case of identical media on both sides of the film, equations (6) reduce to those given by Bell (ref. 8). It can be shown that, in the limit as d approaches zero, equations (6) do not yield the correct single surface reflectance coefficient for a bare substrate. This is the analytic counterpart to the statement made pre-

viously that interference effects must be considered for very thin films.

The double integral over λ and ξ required in equation (4) was evaluated numerically on an IBM 7094 computer. A Simpson rule integration subroutine that was accurate to five significant figures was used. Finite wavelength limits on the λ integration were a minimum of 2 and a maximum of 200 micrometers. These limits effectively cover the wavelength interval of significant energy for 300 K blackbody incident radiation.

The temperature of the radiation source in the experiment of Caren et al. was 290 K. The temperature of the radiation source in Merriam's experiment was 302 K. Both temperatures yielded the same numerical results for total absorptance. Thus, the small temperature difference between the two experiments does not prevent a quantitative comparison of their results.

OPTICAL CONSTANTS

Appropriate optical constants (n, k) of the film and substrate must be chosen to apply the theory. Both polished metal and metal coated with black paint were used for substrates. Considering first the polished surfaces, Caren et al. used polished aluminum whose measured total absorptance for the incident radiation was 0.07 (reflectance, 0.93). Merriam used polished nickel whose measured absorptance was 0.065 (reflectance, 0.935). Although $n(\lambda)$ and $k(\lambda)$ for aluminum and nickel vary considerably in the infrared, the important quantities in the present work are the reflectances obtained from the n, k , and these vary slightly in the infrared (ref. 9). The optical constants of aluminum and nickel were therefore assumed to be equal to each other and independent of λ . This is a greybody assumption. Empirical greybody optical constants n_g, k_g were chosen by finding n_g, k_g such that $R_H = 0.932$, where R_H is the hemispherical reflectance of the bare metal surface. The value of 0.932 represents a compromise between the reflectances of aluminum (0.930) and nickel (0.935). The corresponding absorptance is 0.068. Since the n_g, k_g were assumed to be independent of λ , the total hemispherical reflectance for incident blackbody radiation also will be equal to 0.932.

It is recognized that an infinite number of pairs of n, k yield the same R_H . The approach used herein is to seek pairs that are of the same magnitude as the "handbook" optical constants of aluminum at 10 micrometers.

Two reasonable sets of values are $n_g, k_g = 15, 29$ and $n_g, k_g = 20, 32$, both of which yield the same R_H of 0.932. The calculated reflectance of the ice-covered substrate changed by less than 1 percent when one of the pairs was substituted for the other. Thus, the final results for $R(d)$ are not sensitive to the particular choice of substrate optical constants n, k as long as they yield the correct bare substrate reflectance.

The optical constants of the black-coated substrate were obtained in the same manner. Only the substrate of Caren et al. was considered. The experimental reflectance was 0.14, and the greybody optical constants used were $n_g, k_g = 1.5, 0.517$.

Kislovskii (ref. 10) has measured the optical constants of ice between wavelengths of 2 and 200 micrometers. Figure 2 shows the index of refraction $n(\lambda)$ and figure 3 shows the extinction coefficient $k(\lambda)$ of ice. The values depend strongly on λ so that the greybody assumption used for the substrate is not attempted for the cryodeposit itself.

Before Kislovskii's results can be applied to the present analysis, two important possible limitations to the use of his data must be noted. The first limitation is related to the large temperature difference between the cryodeposit at 77 K and Kislovskii's ice samples at 263 K. The optical constants of dielectrics can have a strong temperature dependence. However, there is some indication that, for ice, this dependence is not too severe (ref. 10). Therefore, it is explicitly assumed herein that the Kislovskii values of n, k are valid at the lower temperature.

The second limitation is related to the difference in density between ice frozen from water (density, 0.917 g/cm^3) and the ice film in the experiments discussed herein (density, 0.49 to 0.63 g/cm^3). Density differences between two samples of a given material can lead to a difference in the optical constants of the two samples. Therefore, the values of the optical constants of bulk ice should be corrected to apply to lower density ice films. There are several ways of doing this, one of which is simply to reduce the extinction coefficient k by the ratio of the density of the ice film to the density of the bulk sample. Merriam, in fact, has calculated $\mathcal{A}(d)$ for his lowest density cryodeposits using this method of correction. On the other hand, the method employed here is a version of that discussed by Heavens (ref. 11) and Aronson et al. (ref. 12). In this method, the Clausius-Mossotti relation (ref. 13) is used to relate the density of the medium to the complex index of refraction of the medium. Thus, if \bar{n}, \bar{k} are the optical constants of a sample of density $\bar{\rho}$ and n, k are the optical constants of a sample of density ρ ,

$$\frac{1}{\bar{\rho}} \frac{(\bar{n} + i\bar{k})^2 - 1}{(\bar{n} + i\bar{k})^2 + 2} = \frac{1}{\rho} \frac{(n + ik)^2 - 1}{(n + ik)^2 + 2} \quad (7)$$

Equation (7) was used to obtain a common set of corrected optical constants for the films of Caren et al. ($\bar{\rho} = 0.63 \text{ g/cm}^3$) and Merriam's films for which $\bar{\rho} = 0.55 \text{ gram per cubic centimeter}$. The corrected n, k denoted by \bar{n}, \bar{k} are shown in figures 2 and 3. Merriam has also obtained films of lower density ($\bar{\rho} = 0.49 \text{ g/cm}^3$) by a slower deposition rate. A different set of optical constants, denoted by $\bar{\bar{n}}, \bar{\bar{k}}$ was obtained for these slowly deposited films. They are also shown in figures 2 and 3. Note that the corrected optical constants are generally of lower magnitude than the bulk values. The positions

of the various maximums and minimums are unchanged.

In the past, Kislovskii's optical constants have been considered to be the best available; however, recently they have been criticized by Irvine and Pollack (ref. 14). Based on a critical review of the existing literature, they present a revised "best available" set of optical constants. Their optical constants are presented in table I and differ significantly from Kislovskii's. Since Kislovskii's data are usually taken as the "standard optical constants," most of the numerical results have been obtained using them. However, for the purposes of comparison, one calculation is presented using the optical constants of Irvine and Pollack.

RESULTS AND DISCUSSION

The absorptance of ice films as a function of thickness has been calculated for a variety of situations. The results for rapidly deposited films and slowly deposited films on polished metal substrates are shown in figures 4 and 5, respectively. The results for the black-painted substrate are plotted in figure 6. The experimental data obtained by Caren et al. and Merriam are also plotted in the relevant figures. The results of the theoretical calculations are discussed, followed by a comparison of theory with experiment.

Theoretical Results

The effect of interference can be seen by comparing results for the same set of n, k and the same substrate. The usual indication of interference, the periodic variation of absorptance as a function of thickness, is absent. The averaging over θ and λ has washed out the "fringes" and resulted in a very smooth variation of absorptance with thickness. For $d \geq 4$ micrometers, the difference between the results obtained for interfering or noninterfering waves is negligible. For $d < 4$ micrometers, interference effects are important if the substrate reflectance is high and are not important for the black-painted substrate. The difference between the interference and noninterference cases is greatest for films approximately 1 micrometer thick on the polished metal substrates. For this situation, the effect of interference is to lower the absorptance by nearly a factor of 2.

As mentioned previously, Merriam has also calculated $\alpha(d)$ for the lowest density cryodeposits assuming no wave interference. His calculational procedure differed from the method described herein in his method of correcting the optical constants of ice for a reduced density and by using only the real part of the complex index of refraction

of ice to compute the vacuum-ice reflection coefficient (r_{1s}, r_{1p}).

Merriam's results are plotted as curve C (fig. 5) and should be compared with curve A obtained with the present analysis. The results of the two calculations agree for d less than 1 micrometer, but for d greater than 1 micrometer, his results are lower than those presented herein. A computer investigation of the discrepancy showed that neither the use of the complete index of refraction nor the different density correction was responsible for the discrepancy. The discrepancy was actually caused by the use of two different extinction coefficient distributions of ice over the wavelength interval from 7 to 10 micrometers. Merriam used an extinction coefficient distribution that was lower than that used in this analysis and thus obtained a smaller value of $\mathcal{A}(d)$. Merriam chose to have $k(\lambda)$ vanish at $\lambda = 8$ micrometers, while the $k(\lambda)$ shown in figure 3 vanishes at $\lambda = 7$ micrometers. The actual zero point is open to interpretation because of the manner in which Kislovskii plots his optical constants. Unfortunately, this zero point occurs near the peak of the 290 K blackbody energy spectrum causing the results to be rather sensitive to the actual value of the extinction coefficient used in this wavelength interval.

The results of the calculation using the set of n, k (corrected for reduced density) given in table I (from ref. 14) are plotted in figure 5 as curve D. The absorptance obtained in this manner is much lower than that predicted by either the analysis of reference 4 (curve C) or that based on figure 3 (curve A).

This comparison of theoretical predictions points out quite clearly that, before any conclusion can be drawn from a quantitative comparison with the experimental data, more accurate optical constants that have been validated must be available for use.

For large values of d ($\geq 100 \mu\text{m}$), the prominent features of the curves in figures 4 and 6 are (1) $\mathcal{A}(d)$ is independent of the substrate absorptance, (2) $\mathcal{A}(d)$ is essentially independent of d , and (3) the corrected optical constants, corresponding to a low-density ice film, yield a slightly higher asymptotic absorptance (curves C and D, fig. 4) than the original optical constants (curves A and B). These features may be understood as follows: for both sets of n, k , the extinction coefficient is nonzero, except for the region near $\lambda = 2$ micrometers, where the energy in an approximately 300 K blackbody spectrum is negligible. Thus, for sufficiently large d , all the radiation refracted into the ice is absorbed before it reaches the substrate; that is, the ice is effectively opaque. The absorptance must therefore be independent of the substrate for large d . In addition, the absorptance is independent of d since it is simply given by 1 minus the reflectance of the vacuum-ice interface. The reflectance of the vacuum-ice interface for low-density ice is smaller than that of the normal-density ice. Thus, more energy is refracted into, and absorbed by, low-density ice than normal ice. The absorptances differ by only about 3 percent for these large thicknesses. This insensitivity to the exact

values of n, k may be the result, in part, of the fact that the reflectance is averaged over both θ and λ .

For smaller values of d ($<20 \mu\text{m}$), the ice film is semitransparent, and most of the radiation refracted into the ice can reach the substrate. Thus, the substrate absorptance is a major factor in determining the absorptance of the cryodeposit complex, a highly absorbing substrate yielding a highly absorbing cryodeposit complex (see fig. 6). On the other hand, a thin cryodeposit on a highly reflecting substrate yields a cryodeposit complex with small absorptance (see figs. 4 and 5), since most of the radiation is reflected through the cryodeposit and into the vacuum. In this case, the absorptance of the cryodeposit complex is mainly the result of absorption of radiation by the cryodeposit, rather than direct absorption by the substrate itself. Low-density ice has a smaller absorption coefficient than normal-density ice. On a highly reflecting substrate, low-density ice will yield a smaller value of the cryodeposit complex absorptance than will normal-density ice on the same substrate. This behavior for d less than 20 micrometers is demonstrated by the difference between curves A and C (fig. 4). The "crossover" thickness, that is, that thickness at which cryodeposits of different densities have equal absorptance, is approximately 20 micrometers.

Now that a specular model of the cryodeposit complex has been analyzed, the effect of voids and rough interfaces can be briefly considered. The most important effect of voids is to scatter radiation out of the cryodeposit, thus lowering the absorptance. For a highly absorbing cryodeposit, this effect is not large because the scattered radiation is mostly reabsorbed before it leaves the cryodeposit.

The effect of surface roughness depends on the details of the surface profile. First, consider the case in which multiple reflections between facets of the vacuum-ice interface do not occur, but the surface is still rough enough to be appreciably nonspecular. Although the distribution of radiation reflected from such a surface is different from that reflected from a smooth surface, the hemispherical reflectance of the two surfaces may have the same value (ref. 15). Therefore, the hemispherical absorptance of a thick ice cryodeposit, which depends only on the properties of the vacuum-ice interface, is not sensitive to a slight roughness of the interface. On the other hand, if a slightly rough surface is one interface of an optically thin film, the hemispherical absorptance (or reflectance) of the thin-film complex is more sensitive to surface roughness. It has already been mentioned that the interference which leads to lower absorptance can be eliminated by surface roughness. The roughness can also allow radiation to propagate in the film in directions outside the cone of refracted radiation allowed by Snell's law of refraction. This results in increased absorptance since these oblique rays have longer paths in the film than the normally refracted rays and thus suffer increased absorption.

Finally, if the profile is irregular enough to allow multiple reflections between surface facets, the absorptance would be greatly increased. Thus, all the effects associated with surface roughness tend to enhance the absorptance.

Comparison With Experiment

The general trends of the experimental data are predicted rather well by the specular analysis. For example, the experimental data presented in figures 4 and 6 indicate that, for $d \geq 100$ micrometers, the absorptance is independent of d and is the same for both polished and black-painted substrates. This behavior agrees with the analysis presented herein for thick ice cryodeposits. Unfortunately, the predicted density dependence of the absorptance of thick cryodeposits noted in the figures cannot be verified because experimental data are lacking for thick cryodeposits of different known densities.

Consider now the question of wave interference. For the rapidly deposited cryodeposits (fig. 4), the theory based on interfering waves (curves A and C) predicts too low an absorptance for d of approximately 1 micrometer. The predictions based on noninterfering waves (curves B and D) are closer to the data. The tentative conclusion to be drawn is that the rapidly deposited films are too uneven to allow the multiply reflected waves to interfere. For the slowly deposited films (fig. 5), the predictions of the interference and noninterference theories (curves A and B) effectively bracket the data for d less than 3 micrometers. Thus, in these cryodeposits it is not possible to state whether or not interference is taking place.

Although the specular analysis has proved adequate to explain the general trends of the experimental data, the overall quantitative agreement is only fair. The discrepancies may be due either to the use of incorrect optical constants of ice in the specular analysis or to nonspecular mechanisms. However, before they are ascribed to nonspecular mechanisms, such as rough interfaces or voids, accurate values of $k(\lambda)$ must be used.

This last point is illustrated by considering the absorptances shown in figure 5 for d in the range from 2 to 10 micrometers. If the values of $k(\lambda)$ presented in figure 3 are valid, curve A is the correct specular prediction and the discrepancy between curve A and the data may be due to the effect of voids which scatter radiation out of the cryodeposit, thus lowering the absorptance. On the other hand, if the extinction coefficients presented in table I are valid, curve D is the correct specular prediction and the discrepancy may be due to surface roughness which raises the absorptance. Finally, if the extinction coefficients used by Merriam are correct, curve C is the correct specular prediction, and the specular hypothesis is consistent with the data.

CONCLUDING REMARKS

The absorption of isotropic 300 K blackbody radiation by ice cryodeposits on metal substrates was analyzed theoretically. The analysis was based on the hypothesis that

the cryodeposit reflected the incident radiation specularly. This specular model of the cryodeposit complex was developed with the equations of classical thin-film optics. The expressions for the monochromatic, unidirectional reflectance took account of both interfering and noninterfering multiply reflected waves. The reflectance (and, hence, absorptance) of the system for the incident isotropic blackbody radiation was obtained by integrating the monochromatic, unidirectional reflectance over wavelength and angle of incidence.

The general features of the existing experimental data were in accord with the theoretical predictions. However, a comparison of theory with experiment did not permit any conclusion to be drawn concerning the detailed optical characteristics of cryodeposits such as specularity, diffuseness, or interference. Before definitive statements concerning these characteristics can be made, both more accurate optical constants, that have been validated, and the proper experimental data must be available. For example, interference effects should be investigated using monochromatic light to allow the appearance of the characteristic fringes and the specularity of cryodeposits should be determined by making biangular reflectance measurements.

Lewis Research Center,
National Aeronautics and Space Administration,
Cleveland, Ohio, February 5, 1969,
124-09-18-04-22.

REFERENCES

1. Wood, B. E.; and Smith, A. M.: Spectral Reflectance of Water and Carbon Dioxide Cryodeposits from 0.36 to 1.15 μ . AIAA J., vol. 6, no. 7, July 1968, pp. 1362-1367.
2. Caren, R. P.; Gilcrest, A. S.; and Zierman, C. A.: Thermal Absorbtances of Cryodeposits for Solar and 290⁰ K Blackbody Sources. Advances in Cryogenic Engineering. Vol. 9. K. D. Timmerhaus, ed., Plenum Press, 1964, pp. 457-463.
3. Young, R. L.; and Todd, D. C.: The Radiative Properties of Cryodeposits Exposed to Infrared Radiation. The Fluid Dynamic Aspects of Space Flight. AGARDograph 87, Vol. 2. Gordon and Breach Science Publ., Inc., 1966, pp. 69-87.
4. Merriam, Richard L.: A Study of Radiative Characteristics of Condensed Gas Deposits on Cold Surfaces. Ph. D. Thesis, Purdue University, June 1968.
5. Tolansky, Samuel: Surface Microtopography. Interscience Publ., Inc., 1960, pp. 19-23.

6. Born, Max; and Wolf, Emil: Principles of Optics. Third ed., Pergamon Press, 1965, pp. 354-355.
7. Stern, Frank: Elementary Theory of the Optical Properties of Solids. Solid State Physics. Vol. 15. Frederick Seitz and David Turnbull, eds., Academic Press, 1963, pp. 299-408.
8. Bell, E. E.: Optical Constants and Their Measurement. Handbuch der Physik. Vol. 25, Pt. II. S. Flügge, ed., Springer-Verlag, Berlin, 1967, p. 50, Eq. 37.2.
9. Hass, Georg: Optical Properties of Metals. American Institute of Physics Handbook. Second ed., Dwight E. Gray, ed., McGraw-Hill Book Co., Inc., 1963, pp. 6-103 to 6-122.
10. Kislovskii, L. D.: Optical Characteristics of Water and Ice in the Infrared and Radiowave Regions of the Spectrum. Optics and Spectr., vol. 7, no. 3, Sept. 1959, pp. 201-203.
11. Heavens, O. S.: Optical Properties of Thin Solid Films. Dover Publ., 1965, pp. 176-178.
12. Aronson, James R.; Emslie, Alfred G.; Allen, Ronald V.; and McLinden, Hugh G.: Studies of the Middle- and Far-Infrared Spectra of Mineral Surfaces for Application in Remote Compositional Mapping of the Moon and Planets. J. Geophys. Res., vol. 72, no. 2, Jan. 15, 1967, pp. 687-703.
13. Panofsky, Wolfgang K. H.; and Phillips, Melba: Classical Electricity and Magnetism. Addison-Wesley Publ. Co., 1955, pp. 33-34.
14. Irvine, William M.; and Pollack, James B.: Infrared Optical Properties of Water and Ice Spheres. Icarus, vol. 8, no. 2, Mar. 1968, pp. 324-360.
15. Bennett, H. E.: Influence of Surface Roughness, Surface Damage, and Oxide Films on Emittance. Thermal Radiation of Solids. NASA SP-55, 1965, pp. 145-152.

TABLE I. - INDEX OF REFRACTION AND EXTINCTION

COEFFICIENT OF ICE (FROM REF. 14)

Wavelength of incident radiation, λ , μm	Index of refraction, n	Extinction coefficient, k	Wavelength of incident radiation, λ , μm	Index of refraction, n	Extinction coefficient, k
2.00	1.291	0.00161	5.5	1.226	.0210
2.05	1.289	.00140	5.6	1.226	.0244
2.10	1.288	.000835	5.7	1.226	.0313
2.15	1.286	.000676	5.8	1.227	.0424
2.20	1.282	.000308	5.9	1.232	.0526
2.25	1.278	.000213	6.0	1.235	0.0617
2.30	1.275	.000198	6.05	1.235	.0646
2.35	1.270	.000350	6.1	1.234	.0643
2.40	1.258	.000571	6.2	1.232	.0616
2.45	1.247	.000707	6.3	1.228	.0584
2.50	1.235	.000795	6.4	1.226	.0555
2.55	1.220	.000850	6.5	1.225	.0551
2.60	1.206	.000802	6.6	1.223	.0559
2.625	1.200	.000835	6.65	1.222	.0564
2.65	1.193	.00143	6.7	1.222	.0554
2.8	1.152	.0123	6.8	1.221	.0535
2.85	1.140	.0353	6.9	1.221	.0508
2.9	1.132	.1014	7.0	1.221	.0491
2.95	1.125	.1805	7.1	1.221	.0473
3.0	1.130	.2273	7.2	1.221	.0453
3.05	1.192	.3178	7.5	1.220	.0399
3.075	1.225	.3428	8.0	1.219	.0369
3.1	1.280	.3252	8.5	1.217	.0352
3.15	1.547	.2502	9.0	1.210	.0365
3.2	1.557	.1562	9.5	1.192	.0310
3.25	1.550	.0900	10	1.152	.0413
3.3	1.530	.0625	10.5	1.195	.0602
3.35	1.515	.0440	11	1.290	.0954
3.4	1.490	.0307	11.5	1.393	.114
3.45	1.445	.0226	12	1.480	.120
3.5	1.422	.0163	12.5	1.565	.119
3.55	1.408	.0129	13	1.612	.108
3.6	1.395	.0105	13.5	1.613	.0935
3.8	1.356	.0082	15	1.550	.0762
3.9	1.340	.0104	17.5	1.486	.0347
4.0	1.327	.0124	20	1.455	.0255
4.1	1.316	.0150	25	1.425	.0298
4.2	1.307	.0175	30	1.427	.0525
4.3	1.299	.0218	35	1.440	.111
4.4	1.288	.0282	40	1.460	.178
4.5	1.280	.0330	43.4	1.49	.321
4.6	1.273	.0287	44.8	1.49	.581
4.7	1.266	.0215	46.5	1.50	.433
4.8	1.258	.0173	52	1.530	.269
4.9	1.252	.0147	56	1.545	.152
5.0	1.247	.0133	62	1.57	.286
5.1	1.241	.0130	83	1.620	.22
5.2	1.236	.0133	100	1.650	.08
5.3	1.231	.0152	117	1.690	.03
5.4	1.227	.0175	150	1.722	.03
			152	1.730	.03

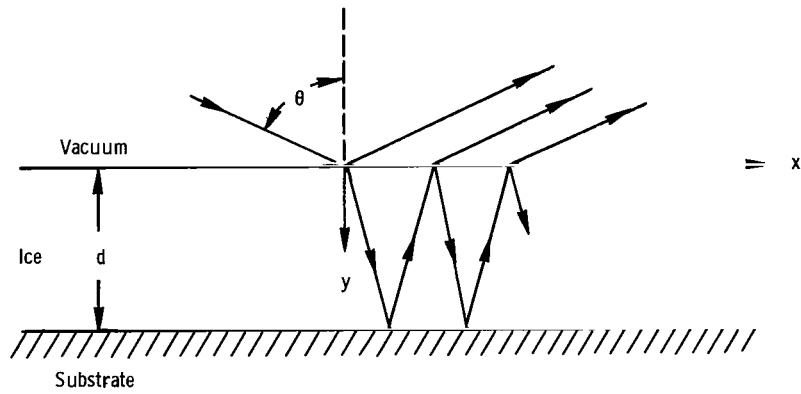


Figure 1. - Model of cryodeposit complex. Also depicted are a few light rays in the cryodeposit.

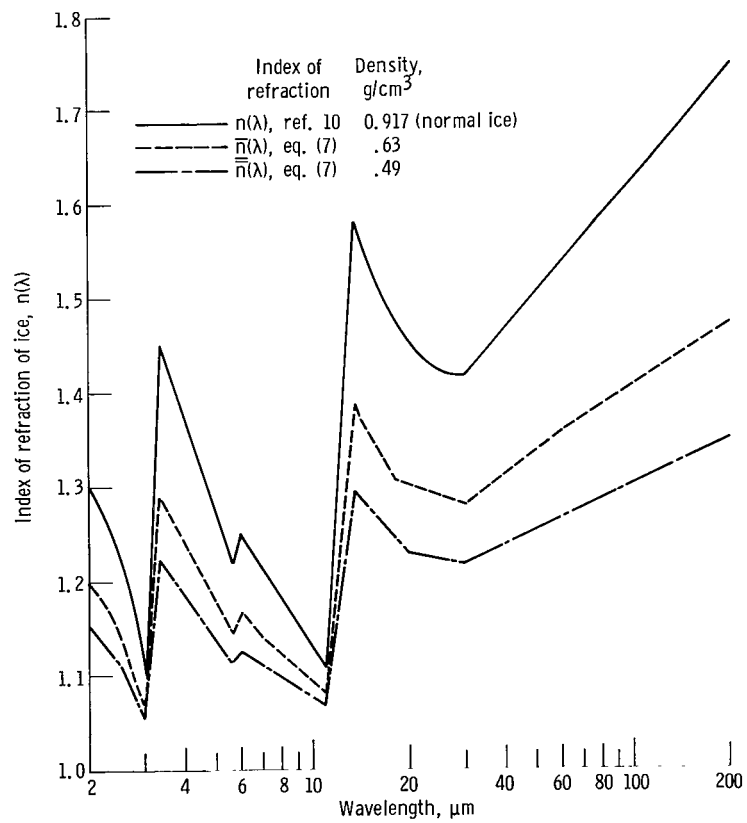


Figure 2. - Index of refraction of ice.

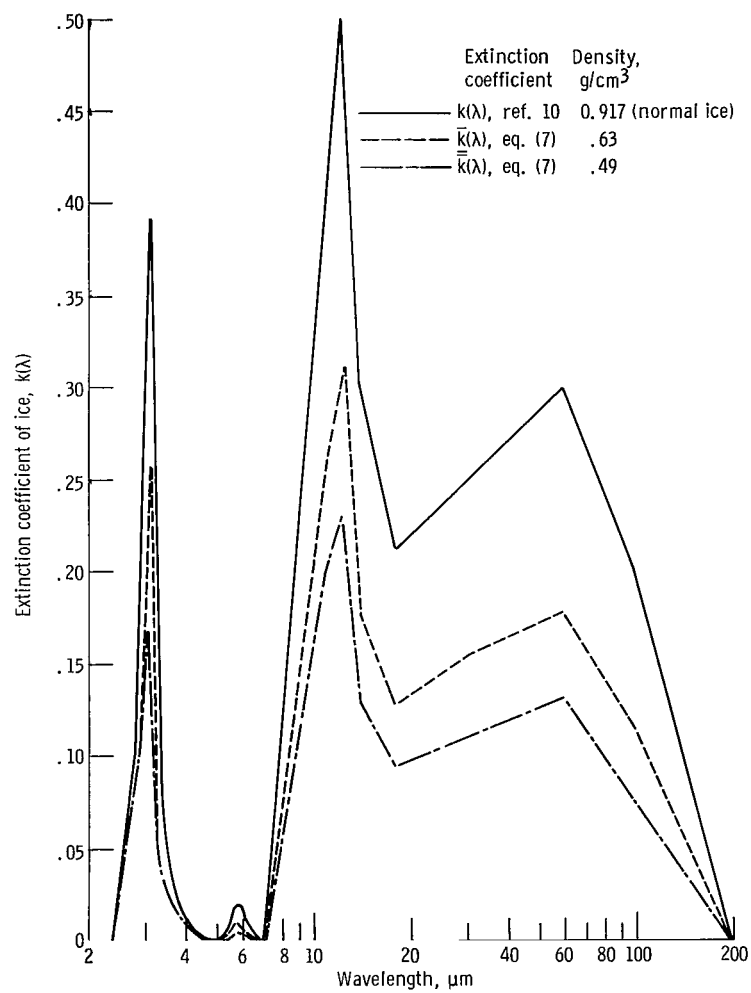


Figure 3. - Extinction coefficient of ice.

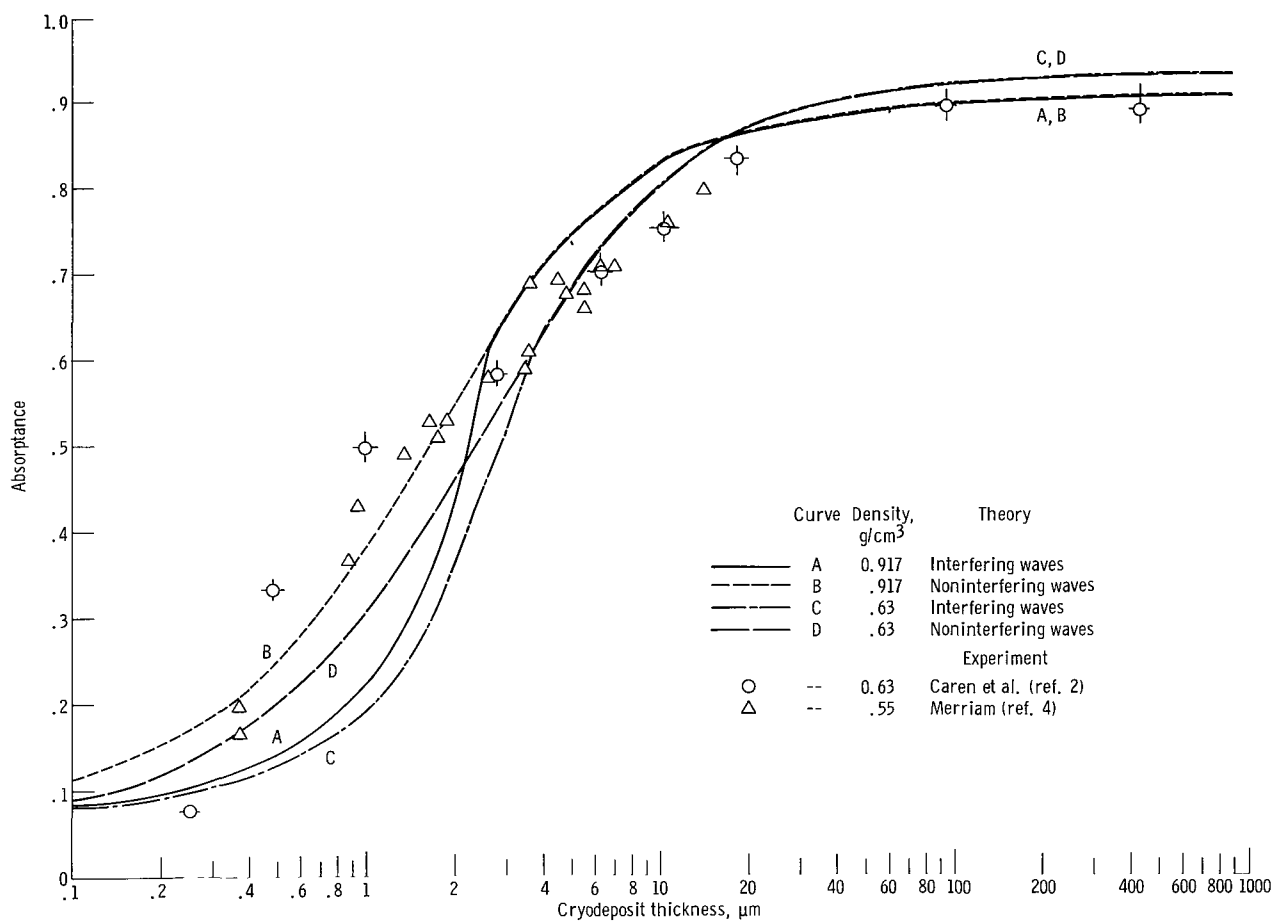


Figure 4. - Absorbance of rapidly deposited ice cryodeposits on polished metal substrate. Experimental data for deposition rate of approximately 20×10^{-7} gram per square centimeter per second. The n, k for all theoretical curves were taken from figures 2 and 3.

ERRATA

NASA Technical Note D-5181

ABSORPTION OF INFRARED RADIATION BY ICE CRYODEPOSITS

by Stephen V. Pepper

April 1969

The following two figures should be added at the end of the report:

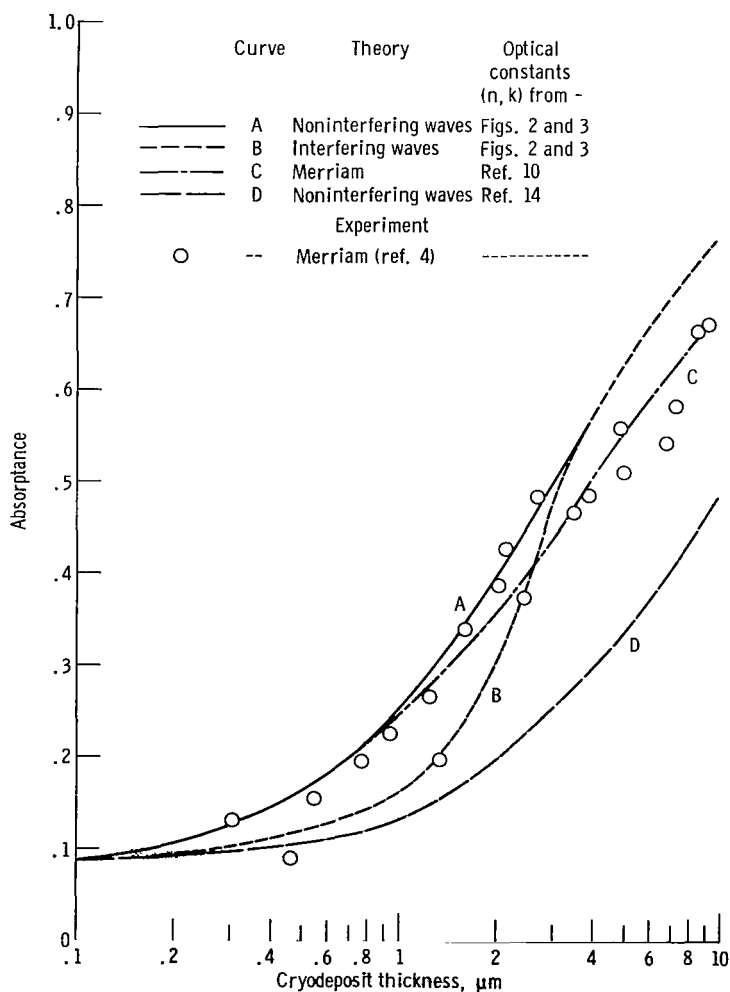


Figure 5. - Absorbance of slowly deposited ice cryodeposits on polished metal (nickel) substrate. Deposition rate, $\sim 10^{-7}$ gram per square centimeter per second; cryodeposit density, 0.49 gram per cubic centimeter.

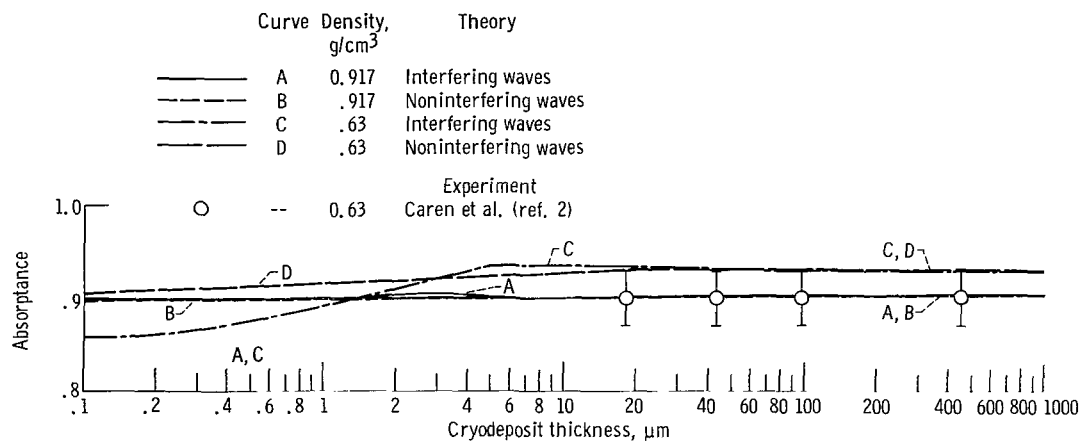


Figure 6. - Absorbance of rapidly deposited ice cryodeposits on blackened metal substrates. Deposition rate, $\sim 20 \times 10^{-7}$ gram per square centimeter per second. The n, k for all theoretical curves were taken from figures 2 and 3.

FIRST CLASS MAIL



POSTMASTER: If Undeliverable (Section 158
Postal Manual) Do Not Return

"The aeronautical and space activities of the United States shall be conducted so as to contribute . . . to the expansion of human knowledge of phenomena in the atmosphere and space. The Administration shall provide for the widest practicable and appropriate dissemination of information concerning its activities and the results thereof."

—NATIONAL AERONAUTICS AND SPACE ACT OF 1958

NASA SCIENTIFIC AND TECHNICAL PUBLICATIONS

TECHNICAL REPORTS: Scientific and technical information considered important, complete, and a lasting contribution to existing knowledge.

TECHNICAL NOTES: Information less broad in scope but nevertheless of importance as a contribution to existing knowledge.

TECHNICAL MEMORANDUMS: Information receiving limited distribution because of preliminary data, security classification, or other reasons.

CONTRACTOR REPORTS: Scientific and technical information generated under a NASA contract or grant and considered an important contribution to existing knowledge.

TECHNICAL TRANSLATIONS: Information published in a foreign language considered to merit NASA distribution in English.

SPECIAL PUBLICATIONS: Information derived from or of value to NASA activities. Publications include conference proceedings, monographs, data compilations, handbooks, sourcebooks, and special bibliographies.

TECHNOLOGY UTILIZATION PUBLICATIONS: Information on technology used by NASA that may be of particular interest in commercial and other non-aerospace applications. Publications include Tech Briefs, Technology Utilization Reports and Notes, and Technology Surveys.

Details on the availability of these publications may be obtained from:

SCIENTIFIC AND TECHNICAL INFORMATION DIVISION
NATIONAL AERONAUTICS AND SPACE ADMINISTRATION
Washington, D.C. 20546